NMR Studies of Echinomycin Bisintercalation Complexes with d(A1-C2-G3-T4) and d(T1-C2-G3-A4) Duplexes in Aqueous Solution: Sequence-Dependent Formation of Hoogsteen A1·T4 and Watson–Crick T1·A4 Base Pairs Flanking the Bisintercalation Site†

Xiaolian Gao and Dinshaw J. Patel*

Department of Biochemistry and Molecular Biophysics, College of Physicians and Surgeons, Columbia University, New York, New York 10032

Received August 20, 1987; Revised Manuscript Received November 2, 1987

ABSTRACT: We report on two-dimensional proton NMR studies of echinomycin complexes with the self-complementary d(A1-C2-G3-T4) and d(T1-C2-G3-A4) duplexes in aqueous solution. The exchangeable and nonexchangeable antibiotic and nucleic acid protons in the 1 echinomycin per tetranucleotide duplex complexes have been assigned from analyses of scalar coupling and distance connectivities in two-dimensional data sets recorded in H_2O and D_2O solution. An analysis of the intermolecular NOE patterns for both complexes combined with large upfield imino proton and large downfield phosphorus complexation chemical shift changes demonstrates that the two quinoxaline chromophores of echinomycin bisintercalate into the minor groove surrounding the dC-dG step of each tetranucleotide duplex. Further, the quinoxaline rings selectively stack between A1 and C2 bases in the d(ACGT) complex and between T1 and C2 bases in the d(TCGA) complex. The intermolecular NOE patterns and the base and sugar proton chemical shifts for residues C2 and G3 are virtually identical for the d(ACGT) and d(TCGA) complexes. A change in sugar pucker from the C2′-endo range to the C3′-endo range is detected at C2 on formation of the d(ACGT) and d(TCGA) complexes. In addition, the sugar ring protons of C2 exhibit upfield shifts and a large 1 ppm separation between the H2′ and H2″ protons for both complexes. The L-Ala amide protons undergo large downfield complexation shifts consistent with their participation in intermolecular hydrogen bonds for both tetranucleotide complexes. A large set of intermolecular contacts established from nuclear Overhauser effects (NOEs) between antibiotic and nucleic acid protons in the echinomycin–tetranucleotide complexes in solution are consistent with corresponding contacts reported for echinomycin–oligonucleotide complexes in the crystalline state [Wang, A. H., Ughetto, G., Quigley, G. J., Hakoshima, T., van der Marel, G. A., van Boom, J. H., & Rich, A. (1984) *Science (Washington, D.C.) 225*, 1115–1121]. We demonstrate that the G·C base pairs adopt Watson–Crick pairing in both d(ACGT) and d(TCGA) complexes in solution. By contrast, the A1·T4 base pairs adopt Hoogsteen pairing for the echinomycin–d(A1-C2-G3-T4) complex while the T1·A4 base pairs adopt Watson–Crick pairing for the echinomycin–d(T1-C2-G3-A4) complex in aqueous solution. These results emphasize the role of sequence in discriminating between Watson–Crick and Hoogsteen pairs at base pairs flanking the echinomycin bisintercalation site in solution.

The quinoxaline family of antibiotics of which echinomycin (Chart I) is a member are powerful antimicrobial and antitumor agents. They consist of two quinoxaline-2-carboxylic acid chromophores attached to a cross-bridged cyclic octapeptide dilactone containing both L- and D-amino acids (Keller-Schierlein et al., 1959). The antitumor effects of the quinoxalines have been attributed to their binding to the DNA of susceptible cells (Ward et al., 1965).

Sedimentation and viscometric studies on the binding of echinomycin to nucleic acids demonstrated that the antibiotic bisintercalates into closed circular DNA at low ionic strength (Waring & Wakelin, 1974). The sequence specificity of echinomycin binding to nucleic acids has been probed with the synthetic cleaving agent methidiumpropyl-EDTA[1]–Fe(II) on restriction fragments (Van Dyke & Dervan, 1984) and by enzymatic cleavage with DNase I and DNase II on the 160 base pair *Escherichia coli* tyr T promotor sequence (Low et al., 1984). These footprinting experiments demonstrate that

Chart I

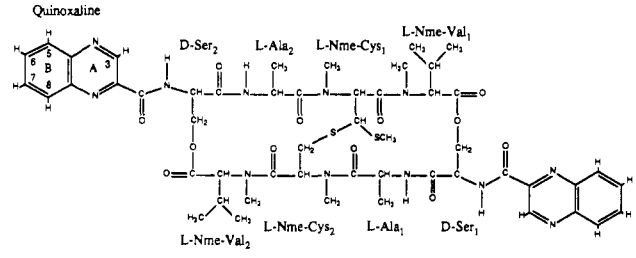

the strongest echinomycin binding sites are centered about dC-dG steps with a site size of four base pairs determined by chemical footprinting (Van Dyke & Dervan, 1984) and six base pairs determined by nuclease footprinting (Low et al., 1984) experiments. Further, hyperreactivity toward DNase (Low et al., 1984) and diethyl pyrocarbonate (Mendel & Dervan, 1987) has been detected in A·T stretches within 5–10 base pairs of the echinomycin binding site.

† This research was supported from start-up funds provided by Columbia University and by NIH Grant CA46778. The NMR spectrometers were purchased from funds donated by the Robert Woods Johnson, Jr., Trust and the Matheson Trust toward setting up the NMR Center in the Basic Medical Sciences at Columbia University.

[1] Abbreviations: EDTA, ethylenediaminetetraacetic acid; DNase, deoxyribonuclease; HPLC, high-performance liquid chromatography; FTNMR, Fourier transform nuclear magnetic resonance; NOE, nuclear Overhauser effect; NMe, *N*-methyl.

0006-2960/88/0427-1744$01.50/0

Our current knowledge of the structural details of the echinomycin–deoxyoligonucleotide complexes is based solely on single-crystal X-ray studies on the d(CGTACG) complex at atomic resolution (Wang et al., 1984). The quinoxaline chromophores of each echinomycin bisintercalate into the minor groove surrounding the dC-dG sequence toward either end of the hexanucleotide duplex. The antibiotic–oligonucleotide complex forms a right-handed helix which is stabilized by intermolecular hydrogen bonding and van der Waals interactions. The observed dC-dG specificity is determined by hydrogen-bonding interactions of alanine residues with the guanosine bases. The A·T base pairs flanking the dC-dG binding site adopt Hoogsteen pairing in the echinomycin–d(CGTACG) complex (Wang et al., 1984). Molecular mechanics calculations on the same complex support formation of Hoogsteen A·T base pairs adjacent to the bisintercalation site (Singh et al., 1986). The hyperreactivity of adenosines to diethyl pyrocarbonate in an echinomycin–DNA restriction fragment complex in solution are also consistent with Hoogsteen A·T base pair formation adjacent to dC-dG bisintercalation sites in solution (Mendel & Dervan, 1987).

We have initiated an NMR research program to investigate echinomycin complexes with stable oligonucleotide duplexes containing dC-dG bisintercalative sites in aqueous solution. The initial challenge was to generate an echinomycin–oligonucleotide complex and solubilize it in aqueous solution at concentrations required for two-dimensional NMR studies. This paper reports on a two-dimensional NMR study of the echinomycin–d(ACGT) and echinomycin–d(TCGA) complexes, which contain purine-C-G-pyrimidine and pyrimidine-C-G-purine binding sites, respectively, in the center of the tetranucleotide duplex.

Experimental Procedures

Oligonucleotide Synthesis. The d(ACGT) tetranucleotide was synthesized by Dr. B. Li of the Middlesex Hospital Medical School. It was purified further by HPLC on a semipreparative reverse-phase C3 column. The d(TCGA) tetranucleotide was synthesized on a 10-μmol scale on a Beckman System 1 plus synthesizer. The general procedures for deprotection and purification by reverse-phase HPLC have been reported previously (Gao & Jones, 1987).

Echinomycin–Oligonucleotide Complex Formation. Two to three equivalents of echinomycin was partially dissolved in 0.5 mL of acetonitrile, and this solution was added to 0.4 mL of an aqueous buffer (0.1 M NaCl, 10 mM phosphate, 0.1 mM EDTA) solution of the tetranucleotide. The mixture was diluted to 5 mL with water and shaken in the cold room for 12 h. Complex formation was monitored by a shift in the oligonucleotide absorption from 260 to 245 nm and the appearance of a weak absorption at 325 nm. The solution was then lyophilized and dissolved in 0.4 mL of water. Excess echinomycin was removed by centrifugation.

We could readily generate the 1 echinomycin per d(ACGT) duplex complex. By contrast, NMR studies had to be undertaken on a 80:20 mixture of a 1 echinomycin per d(TCGA) duplex complex and free d(TCGA) strand.

NMR Sample Preparation. The NMR spectra were recorded on echinomycin–d(ACGT) complex and echinomycin–d(TCGA) complex in a 0.1 M NaCl, 10 mM phosphate, and 0.1 mM EDTA aqueous solution. The d(ACGT) and d(TCGA) concentrations in the complex were 6.3 and 5 mM in duplex, respectively.

NMR Experiments. One- and two-dimensional proton NMR spectra were recorded on a Bruker AM400 spectrometer while phosphorus NMR spectra were recorded on a Bruker AM300 spectrometer. Phosphorus chemical shifts were reported in ppm upfield from external trimethyl phosphate. For two-dimensional spectra recorded in D_2O, the carrier was placed on the HOD resonance and the decoupler channel was used to suppress the residual HOD signal. Two-dimensional data sets were processed by using FTNMR software (Dr. D. Hare, unpublished programs) on VAX 11-780 and micro VAX-II computers using the t_1 noise reduction routines and symmetrized prior to plotting on either ZETA 822 or HP 7475A plotters.

One-dimensional difference NOE experiments were collected in H_2O by using the 1–1 H_2O suppression pulse. The carrier frequency was shifted 4000 Hz downfield from the H_2O resonance and the 1–1 delay optimized for solvent suppression. We collected 2048 complex data points over a 12000-Hz sweep width with a 1.2-s repetition delay. Resonances of interest were irradiated for 400 ms by using the decoupler channel. Data sets corresponding to on- and off-resonance irradiation were interleaved every 32 scans for a total 1600–3200 scans. A line broadening of 3 Hz was applied to the free induction decays which were then subtracted prior to Fourier transformation to obtain the NOE difference spectra.

Correlated spectra (COSY) were recorded in magnitude mode in D_2O solution. Time domain data sets, consisting of 256 t_1 increments, were collected with a sweep width of 4000 Hz by using 1024 complex data points in the t_2 dimension and a repetition delay of 1.5–2 seconds. A total of 32–64 scans were collected for each t_1 increment. The magnitude COSY data were apodized with an unshifted sine bell function in both the t_2 and t_1 dimensions prior to Fourier transformation.

Two-dimensional homonuclear Hartmann–Hahn spectra (HOHAHA) were recorded in D_2O solution on a Bruker AM500 spectrometer. The time domain data sets were accumulated over a sweep width of 5000 Hz by using 1024 and 256 complex data points in t_2 and t_1 dimension, respectively. The spin-lock time was 35 ms, and 64–96 scans were collected for each increment by using a repetition delay of 2 s. The free induction decays were apodized with an unshifted skewed sine bell function in both the t_2 and t_1 dimensions prior to Fourier transformations.

Two-dimensional phase-sensitive NOESY spectra (mixing times 250 and 50 ms) were recorded in D_2O solution. The time domain data sets were accumulated over a sweep width of 4000 Hz by using 1024 complex data points in the t_2 dimension and 256 increments in the t_1 dimension. The repetition delay was 2.0 s, and 32–64 scans were collected for each t_1 increment. The free induction decays were apodized with an unshifted skewed sine bell function in both the t_2 and t_1 dimensions before Fourier transformations. Each dimension was base line corrected with a fifth-order polynomial base line fitting routine supplied by Dr. Arthur Pardi (unpublished program) or Dr. Dennis Hare (unpublished program).

Two-dimensional phase-sensitive NOESY spectra (mixing time 110 ms) in H_2O were recorded by using a jump and return pulse sequence for the preparation, mixing, and detection pulses. The carrier frequency was centered on the H_2O signal and the waiting time t was 90 μs. The time domain data sets consist of 1024 complex data points over a sweep width of 8000 Hz in the t_2 dimension. The repetition delay was 1.0 s. The NOESY data sets in H_2O solution were processed as described for NOESY data sets in D_2O solution, and the data points of water signal were set to zero.

Results

The experiments below were undertaken with the goal of characterizing the mode of binding and the intermolecular

Table I: Proton Chemical Shifts of the Nucleic Acid in Echinomycin Complexes with d(ACGT) and d(TCGA) in H_2O (5 °C) and D_2O (22 °C)

	NH1	NH3	NH_2-4	H8	H2	H6	H5/CH_3	H1′	H2″,2′	H3′	H4′	H5″,5′
	d(ACGT) complex chemical shifts (ppm)[a]											
A1				7.48	7.19			5.85	2.43, 2.31	4.68	4.02	3.63, 3.65
C2			7.58, 6.37			6.78	5.37	5.77	2.03, 1.00	4.34	3.73	4.09, 3.93
G3		11.73		7.93				5.86	2.70, 2.70	4.86	4.17	4.11, 3.94
T4	12.31					7.59	1.79	6.17	2.36, 2.25	4.62	4.06	3.96, 3.96
	d(TCGA) complex chemical shifts (ppm)[b]											
T1	12.80					6.90	1.33	5.70	2.27, 1.87	4.52	3.86	3.68, 3.60
C2			7.66, 6.44			6.83	5.44	5.77	2.03, 1.02	4.39	3.68	4.04, 3.86
G3		11.75		7.93				5.73	2.64, 2.64	4.80	4.16	4.11, 3.90
A4				8.19	7.53			6.25	2.78, 2.45	4.68	4.15	4.00, 3.77

[a] 0.1 M NaCl, 10 mM phosphate, H_2O (pH 6.0), and D_2O (pH 7.0). [b] 0.1 M NaCl, 10 mM phosphate, H_2O (pH 5.9), and D_2O (pH 6.5).

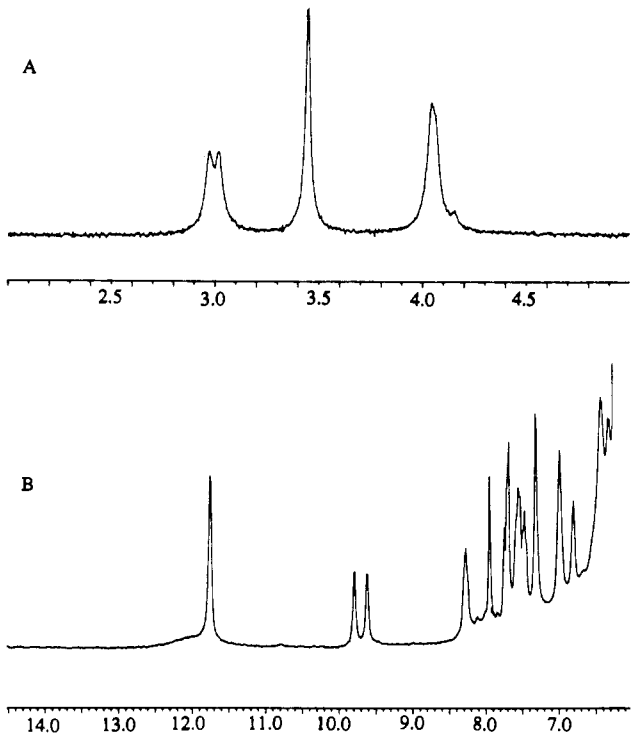

FIGURE 1: Echinomycin–d(ACGT) complex (1 antibiotic per duplex). (A) Proton-decoupled 121-MHz phosphorus NMR spectrum (2–5 ppm upfield from standard trimethyl phosphate) in D_2O buffer, pH 7.0, 25 °C, and (B) 400-MHz proton NMR spectrum (6–14.5 ppm) in H_2O buffer, pH 6.0, 26 °C.

contacts stabilizing the echinomycin–tetranucleotide complexes (1 antibiotic per duplex) in aqueous solution. It was therefore crucial to establish a complete proton assignment of the d(ACGT) and d(TCGA) complexes and then probe structural features from distance-dependent NOE measurements.

Echinomycin–d(ACGT) Complex. The proton-decoupled 121-MHz phosphorus spectra of the echinomycin–d(ACGT) duplex complex in D_2O buffer at 25 °C is plotted in Figure 1A. Echinomycin lacks an exact twofold element of symmetry and removes the twofold symmetry of the tetranucleotide duplex on complex formation. We note that one phosphate resonates at an unperturbed chemical shift of 4.0 ppm while the two remaining phosphates shift downfield on complex formation.

The proton spectra (6.0–14.5 ppm) of the echinomycin–d(ACGT) duplex complex in H_2O buffer at ~26 °C is plotted in Figure 1B. The internal guanosine imino proton exhibits a narrow line width compared to the broad terminal thymidine imino proton in the 11.5–12.5 ppm region at this temperature. In addition, the L-Ala and D-Ser amide protons of echinomycin resonate at ~9.7 ppm and at ~8.1 ppm.

Table II: Proton Chemical Shifts of Drug in Echinomycin Complexes with d(ACGT) and d(TCGA) in H_2O (5 °C) and D_2O (22 °C)

	NH	Hα	Hβ	Hγ	NCH_3	SCH_3
	d(ACGT) complex chemical shifts (ppm)[a]					
L-NMe-Cys(1)		6.41	4.77		2.93	2.06
L-NMe-Cys(2)		5.75	3.40, 2.86		2.96	
L-NMe-Val(1)		4.59	2.36	1.03	3.11	
L-NMe-Val(2)		4.79	2.37	0.97	3.15	
D-Ser(1)	~8.12	5.20	4.44, 4.79			
D-Ser(2)	~8.12	5.22	4.55, 4.79			
L-Ala(1)	9.88	4.82	1.57			
L-Ala(2)	9.70	4.82	1.57			

	Q3	Q5	Q6	Q7	Q8
quinoxaline	7.53	7.35	7.21	6.90	6.92

	NH	Hα	Hβ	Hγ	NCH_3	SCH_3
	d(TCGA) complex chemical shifts (ppm)[b]					
L-NMe-Cys(1)		6.37	4.71		2.87	2.03
L-NMe-Cys(2)		5.72	3.37, 2.78		2.91	
L-NMe-Val(1)		4.39	2.42	1.01, 1.05	3.11	
L-NMe-Val(2)		4.60	2.42	1.01, 1.05	3.17	
D-Ser(1)	~7.96		4.70, 4.21[c]			
D-Ser(2)	~7.96		4.72, 4.13[c]			
L-Ala(1)	9.68	4.77	1.51			
L-Ala(2)	9.51	4.77	1.51			

	Q3	Q5	Q6	Q7	Q8
quinoxaline	7.55	7.61	7.40	7.12	7.23

[a] 0.1 M NaCl, 10 mM phosphate, H_2O (pH 6.0), and D_2O (pH 7.0). [b] 0.1 M NaCl, 10 mM phosphate, H_2O (pH 5.9), and D_2O (pH 6.5). [c] Assignments were made from HOHAHA spectrum at 35 °C, and designations of Ser(1) and Ser(2) are arbitrary.

NOESY Plots of Echinomycin–d(ACGT) Complex in H_2O. A symmetrical contour plot (0.4–12.0 ppm) of the phase-sensitive NOESY spectrum (110-ms mixing time) of the echinomycin–d(ACGT) complex in H_2O buffer at 5 °C is shown in Figure 2A. The cross peaks are well resolved and can be assigned as outlined below. The 11.73 ppm imino proton of G3 exhibits NOEs to the hydrogen-bonded amino protons of C2 (cross peak C, Figure 2A), the amide (cross peaks A, Figure 2A) and CH_3 (cross peak E, Figure 2A) protons of L-Ala, the amide protons of D-Ser (cross peak B, Figure 2A), and the NCH_3 (cross peak D, Figure 2A) and CH_3 (cross peak F, Figure 2A) of L-NMe-Val in the complex. The 9.70 and 9.88 ppm amide protons of L-Ala exhibit NOEs to the imino protons of G3 (cross peak G, Figure 2A), the amide protons of D-Ser (cross peak H, Figure 2A), and the CH_3 protons of L-Ala (cross peak I, Figure 2A) in the complex. The chemical shifts of the nucleic acid imino and amino

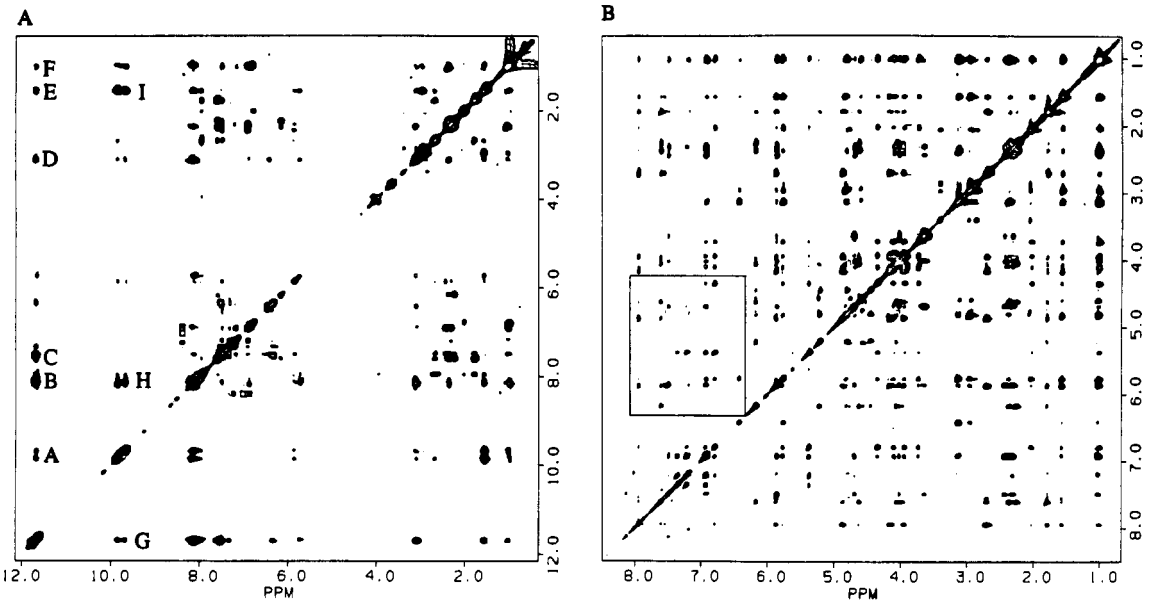

FIGURE 2: (A) Symmetrical contour plot (0–12 ppm) of the phase-sensitive 400-MHz proton NOESY spectrum (110-ms mixing time) of the echinomycin–d(ACGT) complex (1 antibiotic per duplex) in H_2O buffer, pH 6.0, 5 °C. (B) Symmetrical contour plot (0.8–8.5 ppm) of the phase-sensitive 400-MHz proton NOESY spectra (250-ms mixing time) of the echinomycin–d(ACGT) complex (1 antibiotic per duplex) in D_2O buffer, pH 7.0, 22 °C.

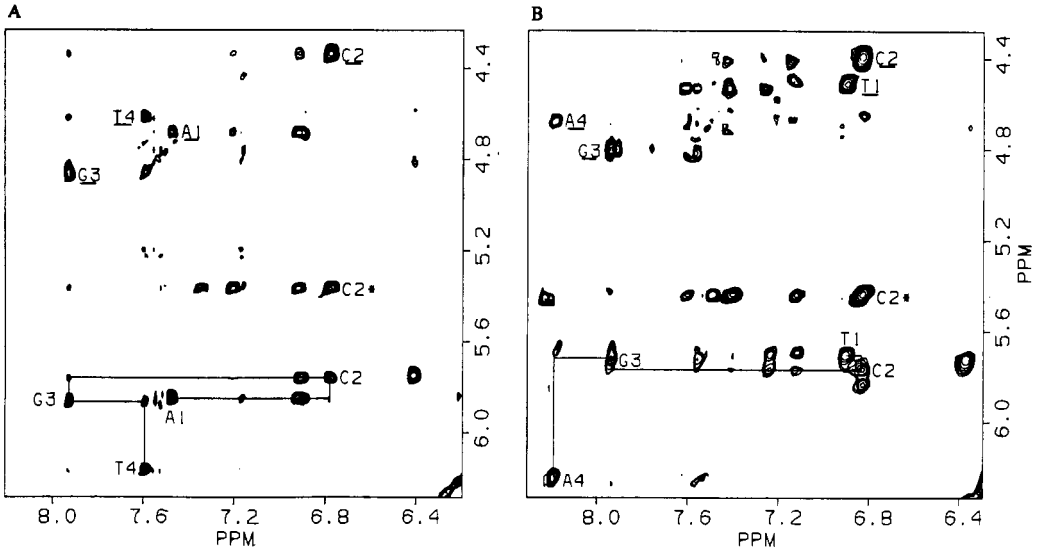

FIGURE 3: Expanded contour plots establishing distance connectivities between the base and quinoxaline protons (6.2–8.2 ppm) and the sugar H1′, H3′, and H5 protons (4.2–6.4 ppm) in the phase-sensitive 400-MHz NOESY spectra (250-ms mixing time) of (A) the echinomycin–d(ACGT) complex (1 antibiotic per duplex) and (B) the echinomycin–d(TCGA) complex (80% 1 antibiotic per duplex, 20% free strand) in D_2O buffer at 22 °C. The cross peaks between the H5 and H6 protons of C2 are designated by an asterisk. The NOEs between the base and their own sugar H1′ protons (5.6–6.4 ppm) and their own sugar H3′ protons (4.3–5.0 ppm) are also labeled in the spectra with the labels for the base–H3′ connectivities underlined.

protons and peptide amide protons in the echinomycin–d(ACGT) complex at 5 °C are listed in Tables I and II, respectively.

NOESY Plots of Echinomycin–d(ACGT) Complex in D_2O. A symmetrical contour plot (0.5–8.5 ppm) of the phase-sensitive NOESY spectrum (250-ms mixing time) of the echinomycin–d(ACGT) complex in D_2O buffer at 22 °C is shown in Figure 2B. An expanded contour plot establishing NOE connectivities between the 6.4–8.2 ppm and the 4.2–6.4 ppm regions along with the cross peak assignments for nucleic acid protons is plotted in Figure 3A. The well-resolved cross peaks for the full NOESY plot in Figure 2B have been completely assigned with the chemical shifts of the nonexchangeable nucleic acid and echinomycin protons in the complex listed in Tables I and II, respectively. These proton spectral assignments were verified by recording and assigning through-bond connectivities in magnitude-correlated (COSY) and phase-sensitive homonuclear Hartmann–Hahn (HOHAHA) two-dimensional NMR experiments in D_2O solution. Stacked plots of the expanded region establishing distance connectivities between the base and quinoxaline protons (6.6–8.2 ppm) and the sugar H1′ and cytidine H5 protons (5.2–6.4 ppm) for NOESY spectra of the d(ACGT) complex at 250- and 50-ms mixing times are plotted in parts A and B, respectively, of Figure 4.

We can monitor a large number of intermolecular NOEs between nonexchangeable protons on the antibiotic and the nucleic acid from an analysis of the NOESY spectrum of the echinomycin–d(ACGT) complex in D_2O solution. These intermolecular distance connectivities are listed as weak, medium, and strong in the compilation summarized in Table III.

Echinomycin–d(TCGA) Complex. Our studies on the echinomycin–d(TCGA) complex were complicated by the presence of 20% free strand in equilibrium with the complex.

Table III: Intermolecular NOEs between Echinomycin and Oligonucleotide Protons in the Echinomycin–d(ACGT) Complex in D_2O at 22 °C[a]

residue	oligonucleotide proton[b]					
	H8, H6	H5/H2	H1′	H3′	H2′,2″	H4′
A1	Q7, Q8 (m) Val-CH_3 (m)		Q7, Q8 (s) Val-CH_3 (s)	Q6 (w) Q7, Q8 (m)	Q7, Q8 (s) Q6 (w)	Q7 (m)
C2	Q6 (w) Q7, Q8 (m) Ala-CH_3 (m) Cys-SCH_3 (m)	Q5 (m) Q6 (s) Q7 (m)	Q7, Q8 (s) Ala-CH_3 (s) Val-CH_3 (m) Cys-SCH_3 (w)	Q6 (w) Q7 (m) Ala-CH_3 (w) Val-CH_3 (w) Cys-SCH_3 (w)	Ala-CH_3 (s)	Q7 (m) Val-CH_3 (m) Cys-SCH_3 (w) Ala-CH_3 (m)
G3	Q3 (w) Ala-CH_3 (m)		Q3 (w) Ser-Hα (w) Ala-CH_3 (s)		Q3 (w) Ser-Hα (w) Ala-CH_3 (m)	Ala-CH_3 (s)
T4			Ser-Hα (s) Ser-Hβ (m)		Ser-Hα (w)	

[a] 0.1 M NaCl, 10 mM phosphate, and D_2O, pH 7.0. [b] The NOEs are designated strong (s), medium (m), and weak (w).

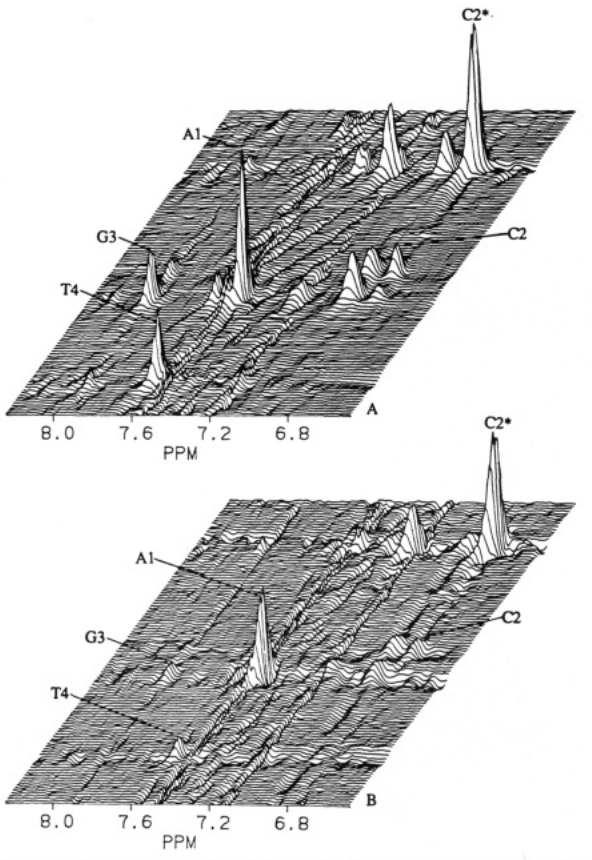

FIGURE 4: Stacked plots establishing distance connectivities between the base and quinoxaline protons (6.6–8.2 ppm) and the sugar H1′ and cytidine H5 protons (5.2–6.3 ppm) in (A) the 250-ms mixing time and (B) the 50-ms mixing time phase-sensitive 400-MHz NOESY spectra of the echinomycin–d(ACGT) complex (1 antibiotic per duplex) in D_2O buffer at 22 °C.

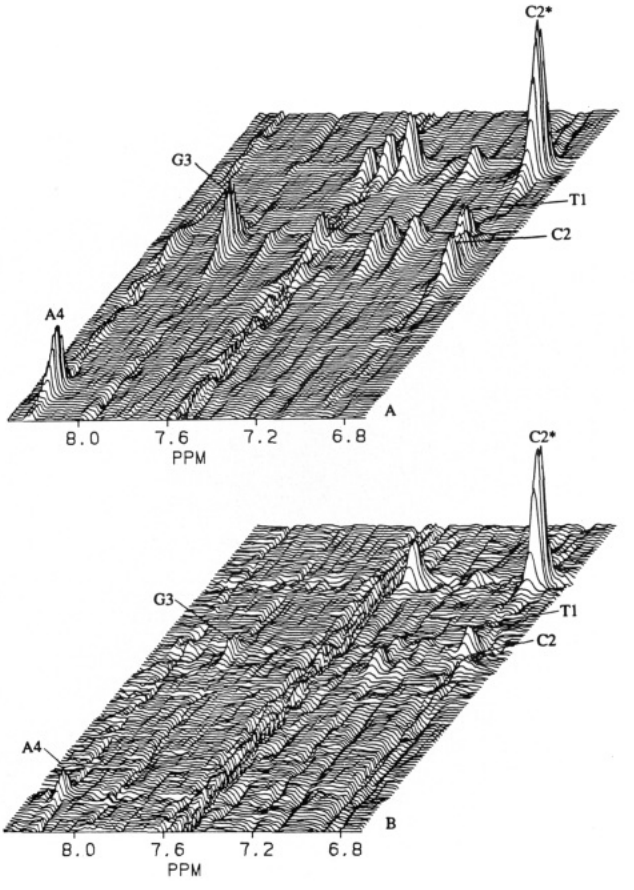

FIGURE 5: Stacked plots establishing distance connectivities between the base and quinoxaline protons (6.6–8.2 ppm) and the sugar H1′ and cytidine H5 protons (5.2–6.4 ppm) in (A) the 250-ms mixing time and (B) the 50-ms mixing time phase-sensitive 400-MHz NOESY spectra of the echinomycin–d(TCGA) complex (80% 1 echinomycin per duplex, 20% free strand) in D_2O buffer at 22 °C.

However, the NOESY spectrum of the complex in D_2O buffer at 22 °C could be readily interpreted, and the proton cross peaks are completely assigned. An expanded contour plot establishing NOE connectivities between the 6.4–8.2 ppm and the 4.2–6.4 ppm regions along with cross peak assignments for nucleic acid protons is plotted in Figure 3B. We also detect exchange cross peaks between free d(TCGA) and the complex that were helpful in confirming the assignments. The assignments of the exchangeable and nonexchangeable protons of the nucleic acid and echinomycin in the d(TCGA) complex are listed in Tables I and II, respectively, and were independently confirmed by through-bond two-dimensional NMR experiments in D_2O solution. Stacked plots of the expanded region establishing distance connectivities between the base and quinoxaline protons (6.6–8.4 ppm) and the sugar H1′ and cytidine H5 protons (5.2–6.4 ppm) for NOESY spectra of the d(TCGA) complex at 250- and 50-ms mixing times are plotted in parts A and B, respectively, of Figure 5.

The intermolecular distance connectivities between nonexchangeable antibiotic and nucleic acid protons for the echinomycin–d(TCGA) complex are summarized in Table IV.

Discussion

Symmetry of the Complexes. The twofold symmetry of the self-complementary d(ACGT) and d(TCGA) tetranucleotide duplexes is partly removed on echinomycin complex formation. Thus, of the three phosphates in the echinomycin–d(ACGT)

Table IV: Intermolecular NOEs between Echinomycin and Oligonucleotide Protons in the Echinomycin–d(TCGA) Complex in D_2O at 22 °C[a]

	oligonucleotide proton[b]					
residue	H8, H6	H5/H2	H1′	H3′	H2′,2″	H4′
T1	Q6, Q7 (w)		Q7, Q8 (w) Val-CH_3 (m)[d]	Q7 (w)	Q6, Q7, Q8 (w) Val-CH_3 (m)[d]	
C2	Q6, Q7 (w) Ala-CH_3 (w)	Q5 (w) Q6 (m) Q7 (w)	Q7, Q8 (w) Ala-Hα (w) Ala-CH_3 (s) Val-CH_3 (m)[d]	Q6 (w) Q7 (m)	Ala-CH_3 (w)	Cys-SCH_3 (w)[c] Ala-CH_3 (w) Val-CH_3 (m)[d]
G3	Q3 (w) Ala-CH_3 (w)		Q3 (w) Ala-CH_3 (s)		Q3 (w) Ala-CH_3 (w)	Ala-CH_3 (m)
A4		Ala-CH_3 (w)	*e*		*e*	

[a] 0.1 M NaCl, 10 mM phosphate, and D_2O, pH 6.5. [b] The NOEs are designated strong (s), medium (m), and weak (w). [c] Cys-SCH_3 overlaps with C2(H2′), preventing definitive NOE assignment. [d] Val-CH_3 overlaps with C2(H2″), preventing definitive NOE assignment. [e] Ser-Hα protons resonate on top of HOD resonance, and predicted NOEs to sugar protons of A4 cannot be detected.

Chart II

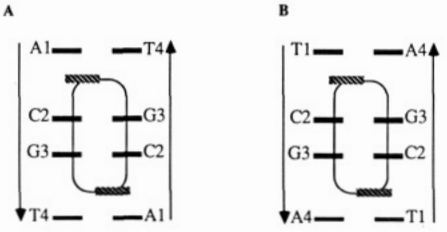

complex, the lowest field resonance at 3.0 ppm exhibits separate peaks, the unshifted resonance at 4.05 ppm exhibits partially overlapping peaks while there is exact superposition of peaks for the low-field resonance at 3.45 ppm (Figure 1A). The resulting proton chemical shift differences are more pronounced between the two halves of echinomycin as reflected in the separate resonances for the resolved L-Ala amide protons (Figure 1B) and the L-NMe-Val and L-NMe-Cys protons for both complexes (Table II).

Bisintercalation. A central feature of the quinoxaline antibiotic–oligonucleotide complex is bisintercalation of the two quinoxaline rings (Waring & Wakelin, 1974) surrounding C-G sites in duplex DNA in the crystalline (Wang et al., 1984) and solution (Van Dyke & Dervan, 1984; Low et al., 1984) states. These observations predict that the quinoxaline rings should intercalate at (A1-C2)·(G3-T4) steps in the echinomycin–d(ACGT) complex (Chart IIA) and at (T1-C2)·(G3-A4) steps in the echinomycin–d(TCGA) complex (Chart IIB).

It has been demonstrated previously that intercalation of actinomycin D at G-C sites in duplex DNA results in downfield shifts of the phosphates at the intercalation site (Patel, 1974; Petersheim et al., 1984). We note that two of the three phosphates in d(ACGT) shift by 1.1 and 0.6 ppm on complex formation (Figure 1A). The observed downfield shifts of 0.75 and 0.5 ppm for two of the three phosphates in the d(TCGA) complex are also consistent with bisintercalation of the echinomycin chromophore into this duplex.

Previous NMR studies on actinomycin complexes (Patel, 1974; Feigon et al., 1984) have demonstrated that intercalation of aromatic chromophores results in upfield shifts of the imino protons of base pairs adjacent to the intercalation site. The guanosine imino proton of the C2·G3 base pair shifts upfield by 1.1 ppm while the thymidine imino proton of the A1·T4 base pair shifts upfield by 0.7 ppm on formation of the echinomycin–d(ACGT) complex. These results are consistent with intercalation of the quinoxaline chromophores of echinomycin between A1·T4 and C2·G3 base pairs corresponding to the (A1-C2)·(G3-T4) steps in the d(ACGT) duplex (Chart IIA). Similar, upfield shifts are detected for the imino protons of the d(TCGA) duplex on echinomycin complex formation consistent with bisintercalation as shown in Chart IIB.

Table V: Intramolecular NOEs among Echinomycin Protons in the Echinomycin–d(ACGT) Complex in D_2O at 22 °C[a]

L-NMe-Cys	L-NMe-Val	D-Ser/Q[b]	L-Ala	L-NMe-Cys
NCH_3	NCH_3	Hα	Hα	NCH_3
Hα	Hα	Hβ	CH_3[c]	Hα
Hβ	Hβ	Q7		Hβ
	CH_3[c]	Q8		SCH_3

[a] The observed NOEs are designated by the lines drawn connecting different protons; NOEs between protons of the same residue are not shown. [b] No NOEs from adjacent peptides to Q3, Q5, or Q6 are observed. [c] An NOE cross peak between Val-CH_3 and Ala-CH_3 was also detected.

Minor Groove Binding. We can distinguish between minor and major groove binding of echinomycin to the tetranucleotide duplexes by analyzing the intermolecular NOEs between the antibiotic CH_3 groups and the nucleic acid sugar protons. The H1′ and H4′ protons of C2 exhibit medium to strong NOEs to the CH_3 groups of L-Ala and L-NMe-Val for the d(ACGT) complex (Table III) and the d(TCGA) complex (Table IV). Similarly, the H1′ and H4′ protons of G3 exhibit medium to strong NOEs to the CH_3 group of L-Ala for both complexes (Tables III and IV). The sugar H1′ and H4′ protons are located in the minor groove, and these observations are consistent with echinomycin binding in the minor groove of the tetranucleotides in aqueous solution, similar to what has been determined in the crystalline state (Wang et al., 1984). These results also establish that the CH_3 groups of L-Ala and L-NMe-Val are on the same nucleic acid binding face of the antibiotic in these complexes consistent with related crystallographic results (Wang et al., 1984).

Echinomycin Conformation in Complexes. The NOESY cross peaks establish a large number of distance connectivities (<5 Å) between adjacent peptide residues of echinomycin in the d(ACGT) complex (Table V). Thus, the quinoxaline Q8 proton exhibits strong NOEs to the Hβ and CH_3 groups of L-NMe-Val residues orienting the quinoxaline ring relative to the peptide backbone. We detect NOEs among the CH_3 group of L-Ala and the CH_3 and NCH_3 groups of L-NMe-Val and L-NMe-Cys indicative of a hydrophobic patch on one face made by the CH_3 groups on adjacent residues of echinomycin in the complex in solution. Finally, we detect an NOE between the 6.41 and 5.57 ppm Hα protons of the two L-NMe-Cys residues which are bridged by the $C\alpha CH_2CH(SCH_3)C\alpha$ linkage of echinomycin. These qualitative distance connectivities between antibiotic protons in the echinomycin–d(ACGT) complex (Table V) and the echinomycin–d(TCGA) complex in solution are consistent with corresponding structural data for related complexes in the crystalline state.

Tetranucleotide Duplex Conformation in Complexes. The observed directionality of the distance connectivities between the base (purine H8 or pyrimidine H6) protons and their own and 5′-flanking sugar H1′, H2′,2″, and H3′ protons (Hare et al., 1983) (Figures 2B and 3A) demonstrates that the d(ACGT) duplex is right-handed in the complex in solution. We also note that the bisintercalation of the quinoxaline ring into the (A1-C2)·(G3-T4) steps (Chart IIA) and the associated unwinding of the helix results in much stronger NOEs between the base protons and their own sugar protons relative to NOEs between the base protons and their 5′-flanking sugar protons (Figure 3A). We can similarly demonstrate that the d(TCGA) duplex is also right-handed in its echinomycin complex in solution (Figure 3B).

Sugar Pucker in Complex. Qualitative conclusions about deviations in the sugar pucker away from the C2′-endo configuration characteristic of B-DNA can be probed by monitoring the NOEs between the base (purine H8 or pyrimidine H6) protons and their own sugar H3′ protons in the echinomycin complexes with d(ACGT) and d(TCGA) in solution. A feature of the C3′-endo pucker is the reduced distance between the base and sugar H3′ protons relative to the corresponding distances in the C2′-endo pucker. We note that the base to their own sugar H3′ NOE cross peaks are stronger than the base to their own sugar H1′ NOE cross peaks for residue C2 in the 250-ms NOESY spectra for the echinomycin–d(ACGT) complex (Figure 3A) and the echinomycin–d(TCGA) complex (Figure 3B). This conclusion is verified by monitoring the corresponding cross peaks in the 50-ms NOESY spectra of the complexes. These results require that the pucker of C2 be in the C3′-endo range for both complexes in solution.

Complexation Chemical Shifts. Bisintercalation of echinomycin into the d(ACGT) duplex results in pronounced conformational perturbations which are reflected in the large observed proton complexation shifts. We note that the H2′, H2″, H3′, and H4′ protons of C2 are upfield from the corresponding values in the other nucleotides for both the d(ACGT) and d(TCGA) complexes (Table I). The most significant values are the 1.0 ppm chemical shift difference between the H2′ and H2″ protons of C2 for both complexes (Table I).

Finally, the quinoxaline Q3 proton resonates at ~9.5 ppm for echinomycin in organic solvents (Cheung et al., 1978; Kyogoku et al., 1981) compared to a value of ~7.54 ppm for the echinomycin complexes with d(ACGT) and d(TCGA) in solution (Table II). This large upfield shift suggests that the quinoxaline Q3 proton stacks over flanking purines at the intercalation site in the complex in solution consistent with overlaps in the echinomycin–d(CGTACG) complex in the crystalline state (Wang et al., 1984).

Intermolecular Hydrogen Bonds. We detect large downfield shifts of the amide protons of L-Ala on proceeding from echinomycin in chloroform (~7.0 ppm) (Cheung et al., 1978) to echinomycin–tetranucleotide complexes in aqueous solution (~9.7 ppm). This ~2.7 ppm downfield complexation shift is indicative of the amide proton of L-Ala participating in hydrogen bonding on complex formation. This result is consistent with the intermolecular hydrogen bond observed between the amide proton of L-Ala and the N3 of guanosine in the X-ray structure of the echinomycin–d(CGTACG) complex (Wang et al., 1984).

Intermolecular van der Waals Contacts. The observed antibiotic–nucleic acid NOEs establish the intermolecular van der Waals contacts that stabilize the complex. These intermolecular NOEs are listed for the echinomycin–d(ACGT) complex in Table III and for the echinomycin–d(TCGA) complex in Table IV. The relative orientation of the quinoxaline ring when intercalated between A1·T4 and C2·G3 base pairs can be estimated from the intermolecular NOEs between the quinoxaline and nucleic acid protons. The predominant NOEs are between the quinoxaline protons and the base and sugar protons of A1 and C2 (Table III), which establishes that the quinoxaline ring stacks predominantly with A1 and C2 and not with G3 and T4 in the echinomycin–d(ACGT) complex in solution (Chart IIA). We also note that the quinoxaline Q6, Q7, and Q8 protons exhibit the majority of the strong intermolecular NOEs to the base and sugar protons of A1 and C2 (Table III), demonstrating that quinoxaline ring B is directed toward the sugar–phosphate backbone in the A1-C2 dinucleotide step.

The observed intermolecular NOEs in the echinomycin–d(TCGA) complex (Table IV) similarly demonstrate that the quinoxaline ring stacks predominantly with the pyrimidines T1 and C2 and not with the purines G3 and A4 (Chart IIB) and that quinoxaline ring B is directed toward the sugar–phosphate backbone in the T1-C2 step for the d(TCGA) complex.

The CH_3 protons of L-Ala exhibit intermolecular NOEs to the base and sugar protons of C2 and G3 in the echinomycin complexes with d(ACGT) (Table III) and with d(TCGA) (Table IV). These distance connectivities establish that the Ala CH_3 group is wedged into the C2-G3 step in the echinomycin–d(ACGT) and echinomycin–d(TCGA) complexes.

Finally, we detect intermolecular NOEs between the Hα and Hβ protons of D-Ser and the sugar H1′, H2′, and H2″ protons of T4 in the echinomycin–d(ACGT) complex (Table III). Thus, the echinomycin D-Ser residue and the sugar ring of the T4 residue are in close proximity in d(ACGT) complex in solution similar to what was detected in the crystalline state.

Overall, the van der Waals intermolecular contacts detected in the single-crystal X-ray analysis of echinomycin bisintercalated about C-G sites in oligonucleotide duplexes (Wang et al., 1984) are retained for the structure of the echinomycin–d(ACGT) complex in solution.

G·C Base Pairing in Complex. An NOE is predicted between the guanosine imino proton and the cytidine amino protons on formation of a Watson–Crick G·C base pair. We observe NOEs between the 11.74 ppm imino proton of G3 and the 7.6 and 6.4 ppm hydrogen-bonded and exposed amino protons of C2 for both the d(ACGT) and d(TCGA) complexes. These results establish formation of Watson–Crick C2·G3 base pairs for both echinomycin complexes consistent with related crystallographic results (Wang et al., 1984).

A·T Base Pairing in Complex. An NOE is predicted from the thymidine imino proton to the adenosine H2 proton for a Watson–Crick A·T base pair and a somewhat weaker NOE to the adenosine H8 proton for a Hoogsteen A·T base pair. This approach has not provided definitive discrimination between Watson–Crick and Hoogsteen A·T base pairs for the echinomycin–tetranucleotide complexes due to superposition of quinoxaline protons with the adenosine H8 and H2 protons.

The glycosidic bond at adenosine is anti in the A(anti)·T(anti) Watson–Crick base pair and is syn in the A(syn)·T(anti) Hoogsteen base pair. Thus, differentiation between syn and anti glycosidic torsion angles at the adenosine residue should elucidate whether the A·T base pair is Watson–Crick or Hoogsteen in the echinomycin–tetranucleotide complexes. A strong H8 to H1′ NOE is predicted for adenosine in the syn orientation (interproton separation ~2.5 Å) while a weak H8

to H1′ NOE is predicated for adenosine in the anti orientation (interproton separation ~3.7 Å) when compared to the NOE between the H5 and H6 protons of cytidine (fixed interproton separation 2.5 Å) (Patel et al., 1982).

Experimentally, we detect a strong NOE between the H8 and H1′ protons of A1 (designated A1) which is of comparable magnitude to the NOE between the H6 and H5 protons of C2 (designated C2*) in NOESY spectra of the echinomycin–d(ACGT) complex recorded at 250- (Figure 4A) and 50-ms (Figure 4B) mixing times. The NOEs between the remaining base and their own sugar H1′ protons (designated C2, G3, and T4) are weak in the complex (Figure 4). These results demonstrate that A1 adopts a syn orientation while C2, G3, and T4 adopt anti orientations consistent with formation of A1·T4 Hoogsteen base pairs in the echinomycin–d(A1-C2-G3-T4) complex.

By contrast, the NOE between the H8 and H1′ protons of A4 is weak (designated A4) as are the remaining NOEs between the base and their own sugar H1′ protons (designated T1, C2, and G3) relative to the NOE between the H5 and H6 protons of C2 (designated C2*) in the echinomycin–d(TCGA) complex at 250- (Figure 5A) and 50-ms (Figure 5B) mixing times. These data demonstrate that the glycosidic torsion angles are anti for T1, C2, G3, and A4, requiring formation of Watson–Crick T1·A4 base pairs in the echinomycin–d-(T1-C2-G3-A4) complex.

These NMR results demonstrate that the sequence flanking the C-G echinomycin bisintercalation site in these tetranucleotide duplexes determines whether the flanking A·T base pairs adopt Hoogsteen pairing as observed in the crystalline state (Wang et al., 1984) and inferred from diethyl pyrocarbonate hyperreactivity solution studies (Mendel & Dervan, 1987) or adopt Watson–Crick pairing.

Intermolecular Stacking. The observation of Hoogsteen A·T pairs in the d(ACGT) complex and Watson–Crick A·T pairs in the d(TCGA) complex may reflect the importance of stacking interactions between the quinoxaline ring and A·T base pairs. The observed intermolecular NOEs establish that the quinoxaline ring stacks on A1 and not T4 for the echinomycin–d(ACGT) complex (Table III, Chart IIA) while the quinoxaline ring stacks on T1 and not A4 for the echinomycin–d(TCGA) complex (Table IV, Chart IIB). These conclusions based on NOE connectivities are supported by the observed complexation chemical shifts for the base protons of the A·T pairs since the H8 and H2 protons of A1 are shifted upfield in the d(ACGT) complex while the H6 and CH_3 protons of T1 are shifted upfield in the d(TCGA) complex. These results suggest that Hoogsteen A1·T4 base pair formation in the echinomycin–d(ACGT) complex may reflect, in part, the importance of intermolecular stacking contributions. Indeed, there is excellent stacking between quinoxaline ring B and the six-membered ring of adenosine in the Hoogsteen A·T base pair for the echinomycin–d(CGTACG) complex in the crystalline state (Wang et al., 1984).

ACKNOWLEDGMENTS

The d(ACGT) tetranucleotide was synthesized and provided by Dr. Ben Li of the Middlesex Hospital Medical School, London. We thank Dr. Keith Fox for providing a generous sample of echinomycin used in these studies.

Registry No. Echinomycin–d(ACGT)$_2$, 112621-43-9; echinomycin–d(TCGA)$_2$, 112621-45-1; echinomycin, 512-64-1.

REFERENCES

Cheung, H. T., Feeney, J., Roberts, G. C. K., Williams, D. H., Ughetto, G., & Waring, M. J. (1978) *J. Am. Chem. Soc. 100*, 46–54.

Feigon, J., Denny, W. A., Leupin, W., & Kearns, D. R. (1984) *J. Med. Chem. 27*, 450–465.

Gao, X., & Jones, R. A. (1987) *J. Am. Chem. Soc. 109*, 3169–3171.

Hare, D. R., Wemmer, D. E., Chou, S. H., Drobny, G., & Reid, B. R. (1983) *J. Mol. Biol. 171*, 319–336.

Keller-Schierlein, W., Mihailovic, M. L., & Prelog, V. (1959) *Helv. Chim. Acta 42*, 305–322.

Kyogoku, Y., Higuchi, N., Watanabe, M., & Kawano, K. (1981) *Biopolymers 20*, 1959–1970.

Low, C. M., Drew, H. R., & Waring, M. J. (1984) *Nucleic Acids Res. 12*, 4865–4879.

Mendel, D., & Dervan, P. (1987) *Proc. Natl. Acad. Sci. U.S.A. 84*, 910–914.

Patel, D. J. (1974) *Biochemistry 13*, 2396–2402.

Patel, D. J., Kozlowski, S. A., Nordheim, A., & Rich, A. (1982) *Proc. Natl. Acad. Sci. U.S.A. 79*, 1413–1417.

Petersheim, M., Mehdi, S., & Gerlt, J. A. (1984) *J. Am. Chem. Soc. 106*, 439–440.

Singh, U. C., Pattabiraman, N., Langridge, R., & Kollman, P. A. (1986) *Proc. Natl. Acad. Sci. U.S.A. 83*, 6402–6406.

Van Dyke, M. M., & Dervan, P. B. (1984) *Science (Washington, D.C.) 225*, 1122–1127.

Wang, A. H., Ughetto, G., Quigley, G. J., Hakoshima, T., van der Marel, G. A., van Boom, J. H., & Rich, A. (1984) *Science (Washington, D.C.) 225*, 1115–1121.

Ward, D., Reich, E., & Goldberg, I. H. (1965) *Science (Washington, D.C.) 149*, 1259–1263.

Waring, M. J., & Wakelin, L. P. (1974) *Nature (London) 252*, 653–657.